Selective Photocatalytic Oxidation of (hetro) aryl alcohols to aldehydes and ketones by Visible-Light-Absorbing three-dimensional Ni/ZnO nanoparticles

Zahra bazyar ,[a*]Fatemeh Zeraatpisheh,[a] and Nastaran Moalemiyan, [a]

[a] *Department of Chemistry, Behbahan Khatam Alanbia University of Technology, Behbahan, 63616-63973, I. R. Iran*

Z.bazyar@bkatu.ac.ir

bazyarzahra@yahoo.com

General information

The chemical materials utilized in this study were obtained from Sigma-Aldrich, Fluka, and Merck. The progression of the reactions was monitored using thin-layer chromatography (TLC). Infrared spectra of the samples were obtained using a Bruker FTIR-Tensor II spectrophotometer. The quantity of nickel nanoparticles catalyst (Ni/ZnO) was determined using inductively coupled plasma (ICP). Surface morphologies and microstructures were examined using field emission scanning electron microscopy (FE-SEM, TESCAN MIRA2) and transmission electron microscopy (TEM, Philips EM 208S). Phase composition was determined with a Philips PW1730 XRD instrument in the 2θ range of 20° to 80° at room temperature. BET surface areas of the catalyst were analyzed through nitrogen adsorption at 77 K using a BET BELSORP Mini II. Elemental analysis was conducted with a Thermo Finnigan Flash EA-1112 CHNS analyzer. UV–vis diffuse reflectance spectrum was performed with a PERKIN ELMER LAMBDA 365 spectrophotometer. ^{1}H and ^{13}C NMR spectra were recorded on Bruker, Avance 400 (at 400 MHz, 376 MHz, and 100 MHz respectively).

Table S1. Results BET for three-dimensional Ni/ZnO nanoparticles

Surface area	BET surface area ($m^2.g^{-1}$)	31.928
	BJH adsorption cumulative surface area of pores ($m^2.g^{-1}$)	42.073
Pore size	Mean pore diameter (nm)	39.175
	Pore size distribution (nm)	7.98
Pore volume	Single point adsorption total pore volume of pores ($cm^3.g^{-1}$)	0.3127
	BJH adsorption cumulative volume of pores ($cm^3.g^{-1}$)	0.3193

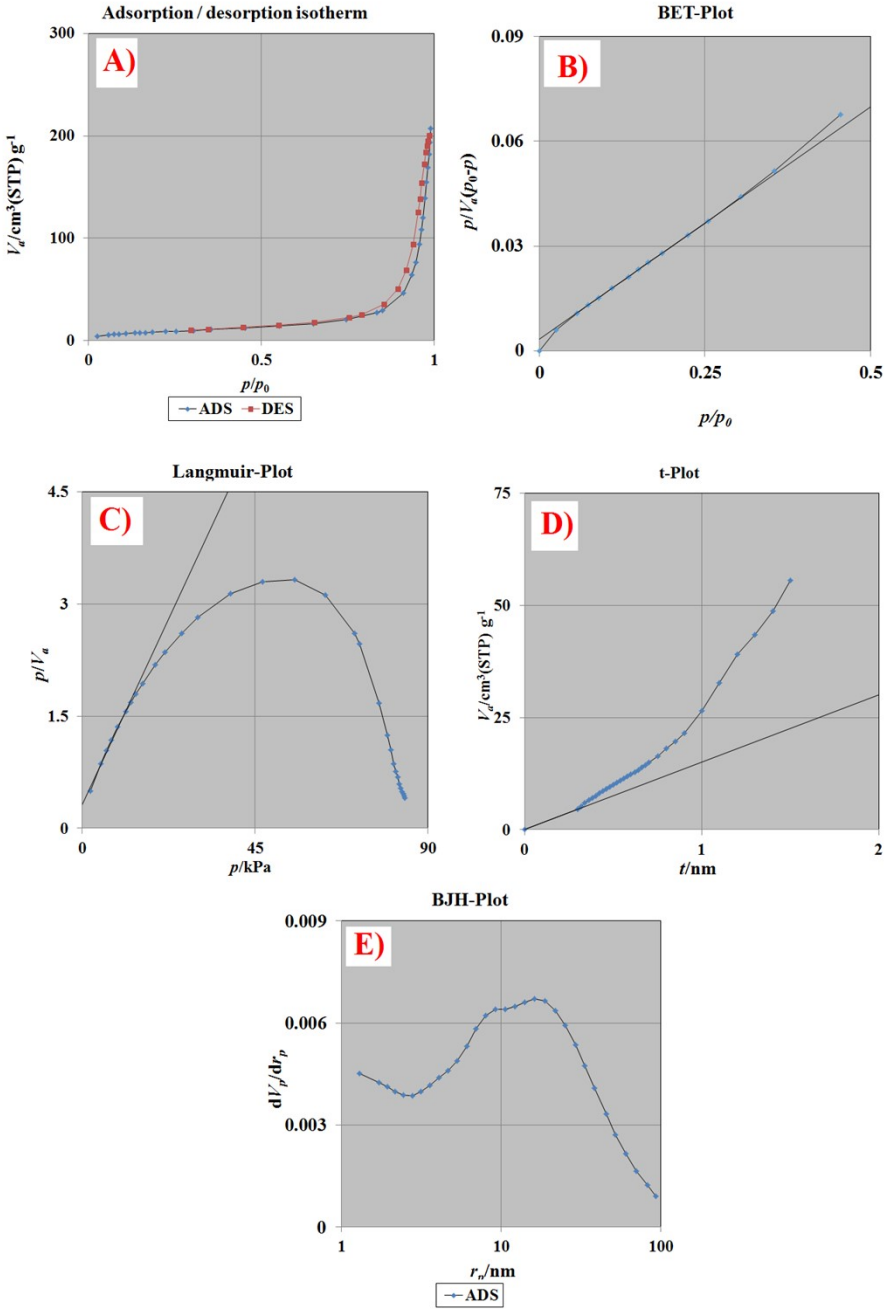

Fig. S1. A) Adsorption/desorption isotherm, **B)** BET Plot, **C)** Langmuir Plot, **D)** t-Plot, **E)** BJH-Plot of Ni/ZnO nanoparticles

\

Characterization data:

4-Methoxybenzaldehyde [1]

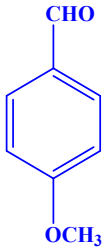

Clear liquid; FT-IR (thin film): ν (cm^{-1}) = 3062, 2965, 2942, 2843, 2729, 1701, 1678, 1519, 1469, 1440, 1382, 1136 cm^{-1}; ^1H NMR (400 MHz, $CDCl_3$) δ (ppm) = 9.80 (s, 1H), 7.79-7.77 (d, 2H, J = 8 Hz,), 6.96-6.92 (d, 2H, J = 8 Hz), 3.83 (s, 3H); ^{13}CNMR (100 MHz, $CDCl_3$,) δ (ppm) = 190.62, 164.60, 131.78, 129.99, 114.38, 55.36.

3, 5-Dimethoxybenzaldehyde [2]

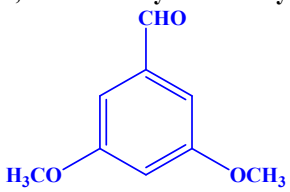

Colorless solid, m.p: 44-48 ˚C (lit. 45-48 ˚C); FT-IR (thin film): ν (cm^{-1}) = 3049, 2971, 2929, 2837, 2814, 1708, 1610, 1582, 1468, 1429, 1381, 1268, 1149, 1028 cm^{-1}; ^1H NMR (400 MHz, $CDCl_3$) δ (ppm) = 9.91 (s, 1H), 7.01 (s, 2H), 6.71 (s, 1H), 3.85 (s, 6H); ^{13}CNMR (100 MHz, $CDCl_3$,) δ (ppm) = 191.93, 161.24, 138.22, 107.14, 107.10, 55.61; Anal. Calcd for $C_9H_{10}O_3$: C, 65.05; H, 6.07. Found: C, 65.09; H, 5.94.

4-Chlorobenzaldehyde [3]

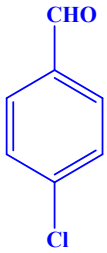

White solid, m.p: 47-48 ˚C (lit. 47.5 ˚C); FT-IR (thin film): ν (cm^{-1}) = 3071, 2857, 2756, 1683, 1579, 1478, 1384, 1286, 1200, 1146, 1083, 811, 699, 533 cm^{-1}; ^1H NMR (400 MHz, $CDCl_3$) δ (ppm) = 9.99 (s, 1H), 7.85-7.82 (d, 2H, J = 8 Hz), 7.54-7.51 (d, 2H, J = 8 Hz); ^{13}CNMR (100 MHz, $CDCl_3$,) δ (ppm) = 191.03, 141.04, 134.70, 131.22, 129.56; Anal. Calcd for C_7H_5ClO: C, 59.81; H, 3.59. Found: C, 59.80; H, 3.52.

2-Nitrobenzaldehyde [1]

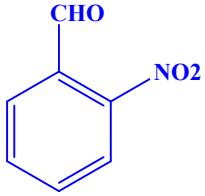

Slightly yellow powder, m.p: 42-43 ˚C (lit. 43 ˚C); FT-IR (thin film): ν (cm^{-1}) = 3068, 2856, 2741, 1699, 1636, 1564, 1502, 1464, 1439, 1316, 1221, 1105 cm^{-1}; ^1H NMR (400 MHz, $CDCl_3$) δ (ppm) = 10.42 (s, 1H), 8.13-8.11 (d, 1H, J = 8 Hz), 7.96-7.94 (d, 1H, J = 8 Hz), 7.82-7.78 (m, 2H); ^{13}CNMR (100 MHz, $CDCl_3$,) δ (ppm) =188.25, 134.02, 133.74, 131.40, 129.79, 124.42; Anal. Calcd for $C_7H_5NO_3$: C, 55.64; H, 3.34; N, 9.27. Found: C, 55.89; H, 3.19; N, 9.31.

3-Nitrobenzaldehyde [4]

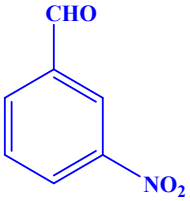

Slightly yellow powder, m.p: 58 ˚C (lit. 58 ˚C); FT-IR (thin film): ν (cm^{-1}) = 3072, 2862, 2729, 1719, 1606, 1559, 1461, 1359, 1254, 1131 cm^{-1}; ^1H NMR (400 MHz, $CDCl_3$) δ (ppm) = 10.14 (s, 1H), 8.73 (s, 1H), 8.52-8.49 (d, 1H, J = 12 Hz), 8.27-8.24 (d, 1H, J = 12 Hz), 7.81-7.77 (t, 1H, J = 8 Hz); ^{13}CNMR (100 MHz, $CDCl_3$,) δ (ppm) = 189.77, 148.77, 137.39, 134.69, 130.42, 128.60, 124.45; Anal. Calcd for $C_7H_5NO_3$: C, 55.64; H, 3.34. Found: C, 55.48; H, 3.74.

4-Formylbenzonitrile [5]

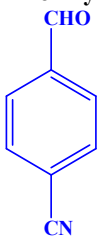

White solid, m.p: 100-102.5 ˚C (lit. 100-102.5 ˚C); FT-IR (thin film): ν (cm^{-1}) = 3049, 2827, 2759, 2234, 1738, 1611, 1545, 1517, 1276, 1168 cm^{-1}; ^1H NMR (400 MHz, $CDCl_3$, ppm) δ 10.11 (s, 1H), 8.02-8.00 (d, 2H, J= 8 Hz), 7.87-7.85 (d, 2H, J= 8 Hz); ^{13}CNMR (100 MHz, $CDCl_3$,) δ (ppm) =190.67, 138.73, 132.92, 129.90, 117.74, 117.59; Anal. Calcd for C_8H_5NO: C, 73.27; H, 3.84; N, 10.68. Found: C, 73.30; H, 3.81; 10.68.

4-Nitrobenzaldehyde [1]

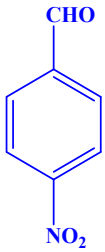

Slightly yellow powder, m.p: 104-106 ˚C (lit. 103-106 ˚C); FT-IR (thin film): ν (cm^{-1}) = 3087, 2876, 2786, 1703, 1676, 1602, 1587, 1544, 1459, 1457, 1410, 1373, 1335, 1287, 1248, 1197, 1124, 1098 cm^{-1}; ^1H NMR (400 MHz, $CDCl_3$) δ (ppm) = 10.18 (s, 1H), 8.43-8.40 (d, 2H, J= 12 Hz), 8.12-8.08 (d, 2H, J= 12 Hz); ^{13}CNMR (100 MHz, $CDCl_3$,) δ (ppm) = 190.32, 151.13, 140.16, 130.50, 124.32; Anal. Calcd for $C_7H_5NO_3$: C, 55.64; H, 3.34; N, 9.27. Found: C, 55.59; H, 3.37; N, 9.17.

Picolinaldehyde [6]

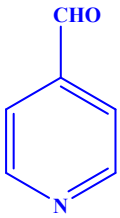

Brown liquid; FT-IR (thin film): ν (cm^{-1}) =3067, 2883, 2726, 1716, 1617, 1547, 1519, 1426, 1321 cm^{-1}; ^{1}H NMR (400 MHz, $CDCl_3$) δ (ppm) =10.06 (s, 1H), 8.78-8.76 (d, 1H, *J*= 8 Hz), 7.95-7.93 (d, 1H, *J*= 8 Hz), 7.90-7.88 (t, 1H, *J*= 4 Hz), 7.54-7.50 (m, 1H); ^{13}CNMR (100 MHz, $CDCl_3$,) δ (ppm) =194.01, 153.10, 150.16, 136.86, 128.00, 122.07;

Furan-2-carbaldehyde [7]

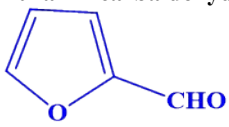

Colorless liquid; FT-IR (thin film): ν (cm^{-1}) =3065, 2846, 2768, 1702, 1678, 1565, 1474, 1392, 1221, 1154, 1061, cm^{-1}; ^{1}H NMR (400 MHz, $CDCl_3$) δ (ppm) =9.87 (s, 1H), 7.74-7.72 (d, 1H, *J*= 8 Hz), 7.71-7.70 (t, 1H, *J*= 8 Hz), 7.16-7.15 (d, 1H, *J*= 8 Hz); ^{13}CNMR (100 MHz, $CDCl_3$,) δ (ppm) =183.09, 143.93, 136.58, 135.19, 128.43.

1*H*-Indole-2-carbaldehyde [8]

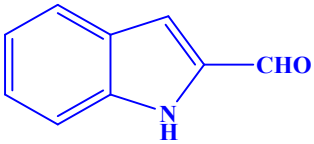

Clear yellow solid, m.p: 197-198 ˚C (lit. 197-198 ˚C); FT-IR (thin film): ν (cm^{-1}) = 3058, 2852, 2754, 1702, 1515, 1437, 1372, 1149 cm^{-1}; ^{1}H NMR (400 MHz, $CDCl_3$) δ (ppm) =11.33 (s, 1H), 9.85 (s, 1H), 8.11-8.09 (d, 1H, *J*= 8 Hz), 7.71 (s, 1H), 7.33-7.28 (m, 1H), 7.14-7.10 (m, 2H); ^{13}CNMR (100 MHz, $CDCl_3$,) δ (ppm) =185.13, 136.84, 124.42, 123.69, 122.24, 121.39, 118.72, 112.11; Anal. Calcd for C_9H_7NO: C, 74.47; H, 4.86; N, 9.95. Found: C, 74.21; H, 4.92; N, 9.87.

III. Spectra

A) ^{1}H, ^{13}C NMR spectra:

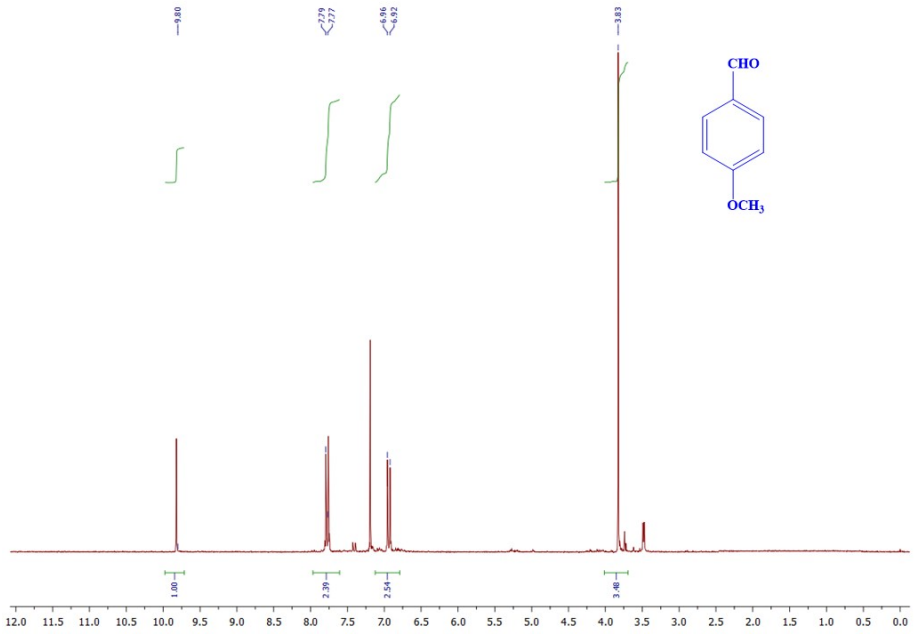

Figure S2.^{1}H NMR spectra of **4-methoxybenzaldehyde** in $CDCl_3$.

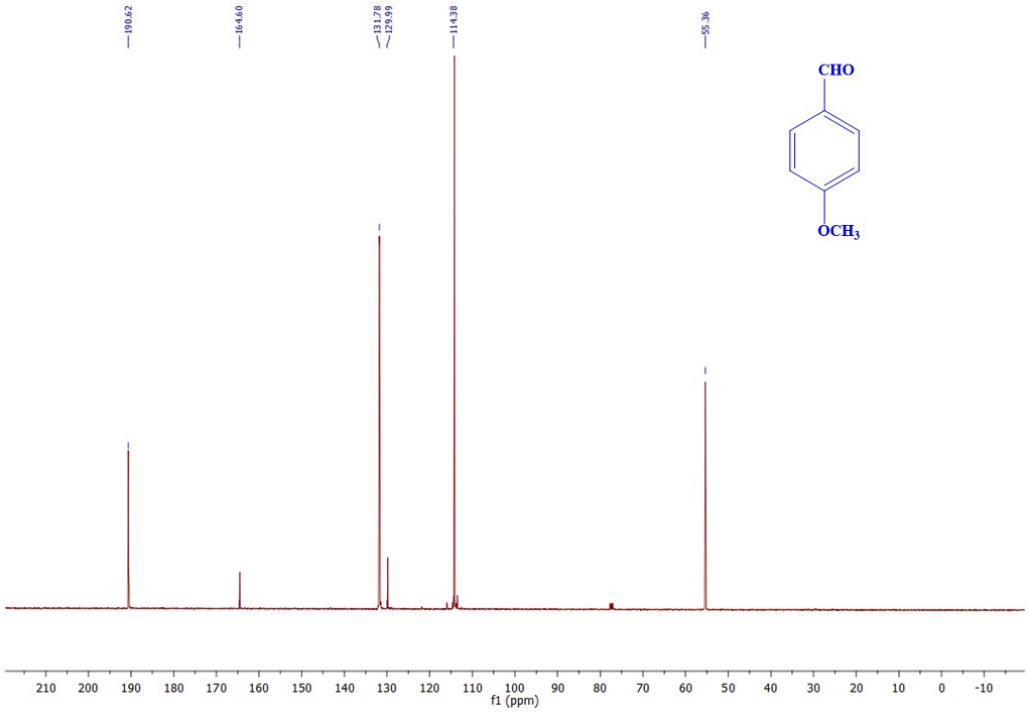

Figure S3.^{13}C NMR spectra of **4-methoxybenzaldehyde** in $CDCl_3$.

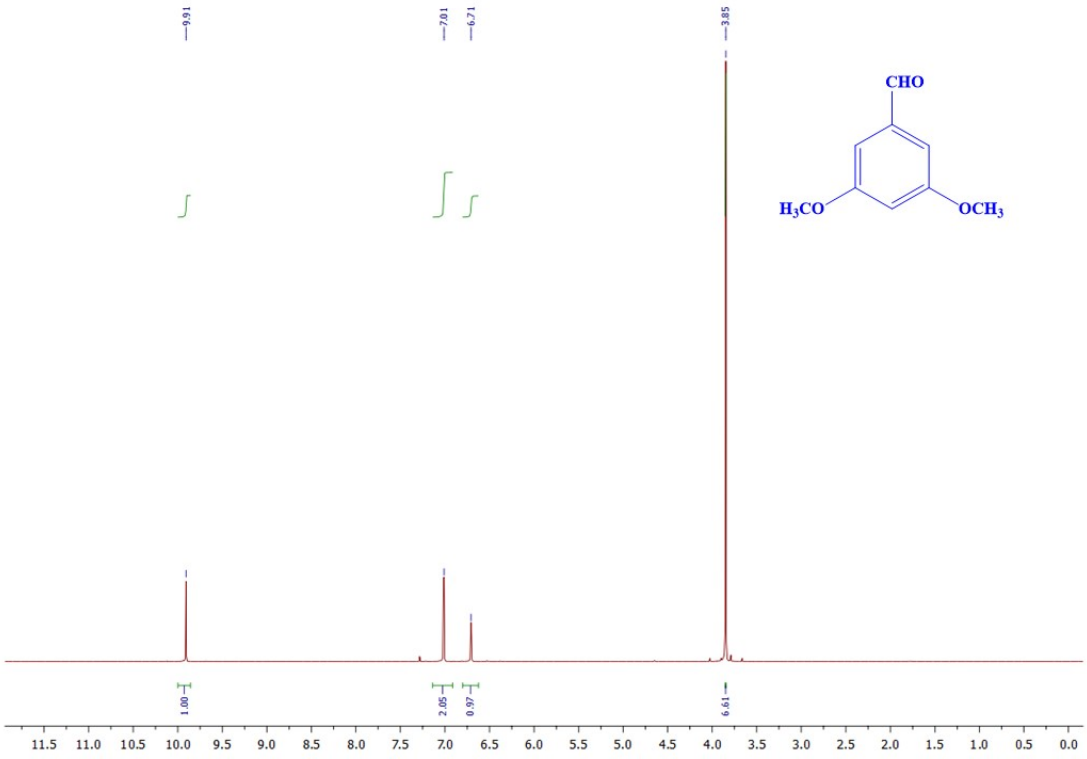

Figure S4. ^{1}H NMR spectra of **3,5-dimethoxybenzaldehyde** in $CDCl_3$.

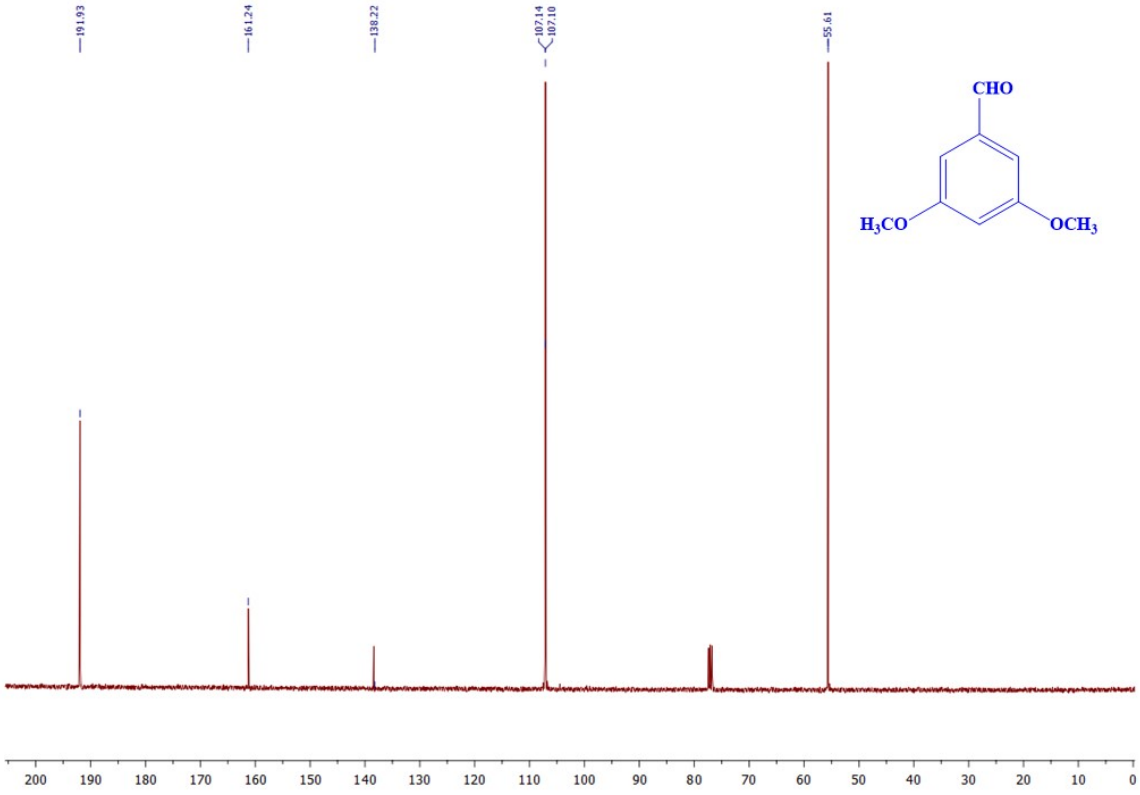

Figure S5. ^{13}C NMR spectra of **3,5-dimethoxybenzaldehyde** in $CDCl_3$.

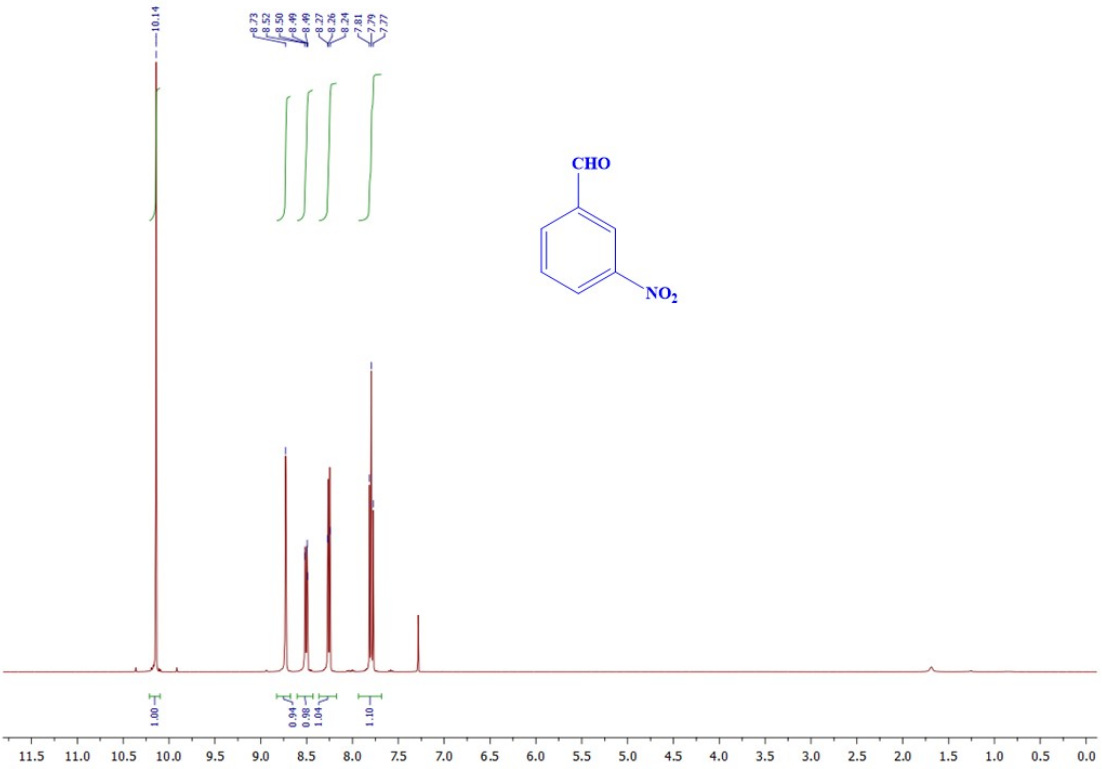

Figure S6.[1]H NMR spectra of **3-nitrobenzaldehyde** in $CDCl_3$.

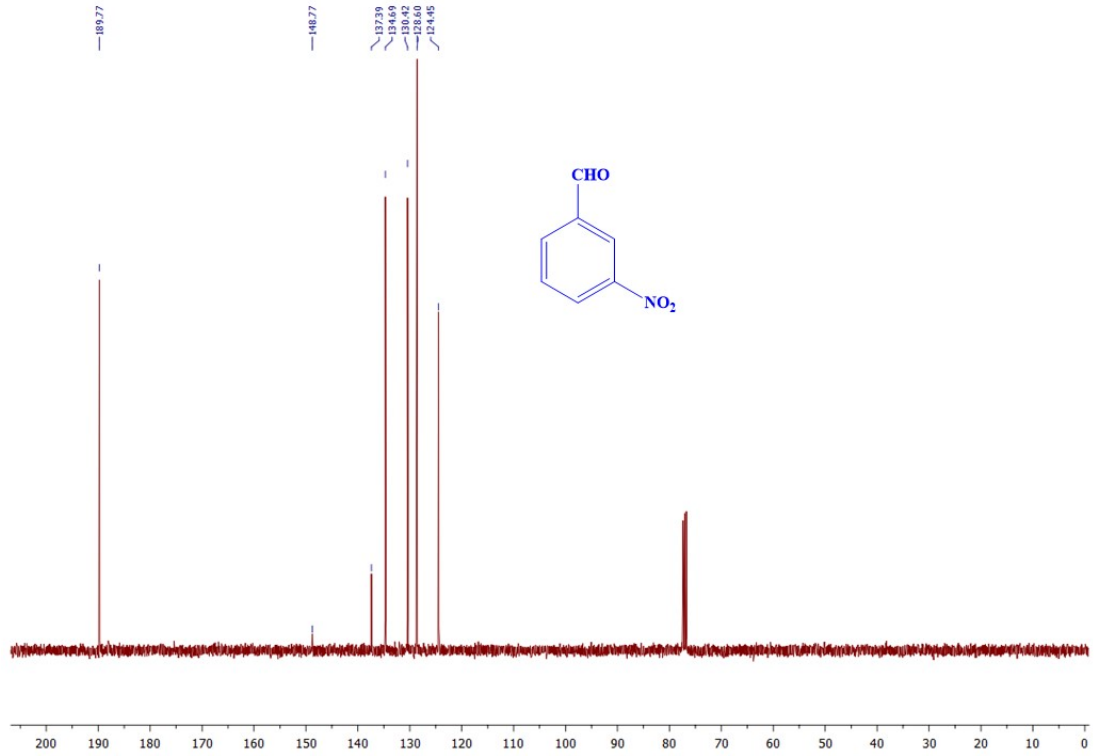

Figure S7.[13]C NMR spectra of **3-nitrobenzaldehyde** in $CDCl_3$.

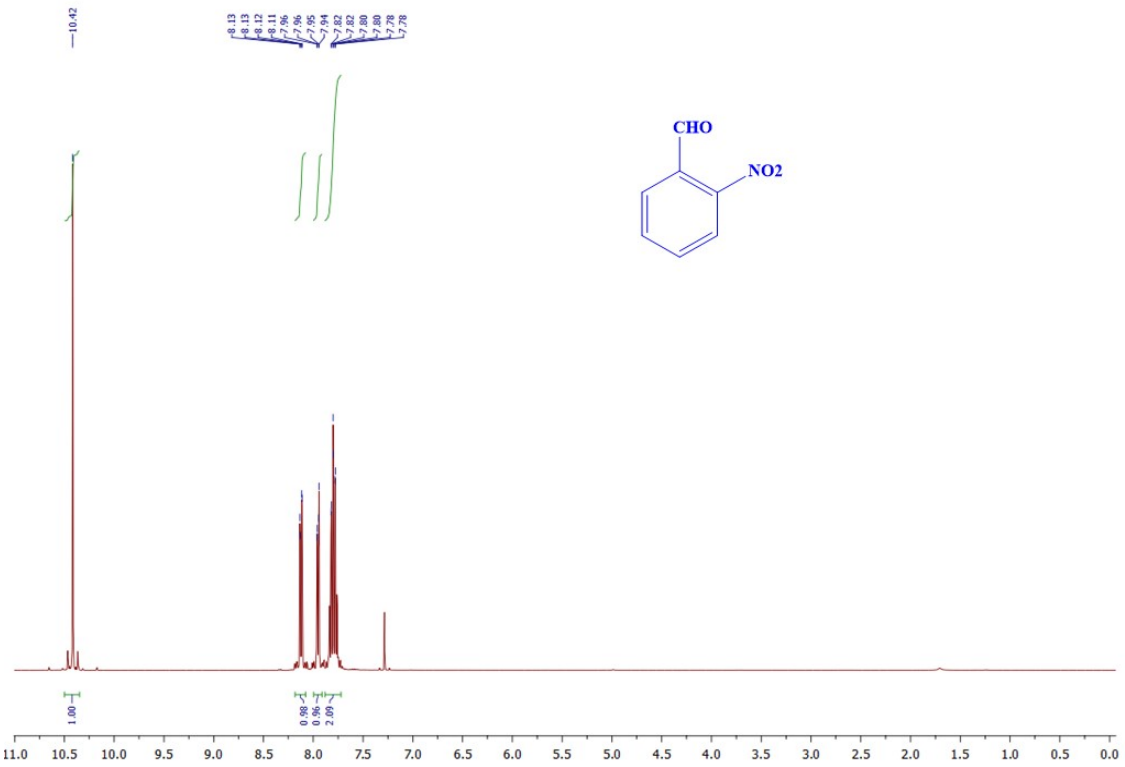

Figure S8.[1]H NMR spectra of **2-nitrobenzaldehyde** in $CDCl_3$.

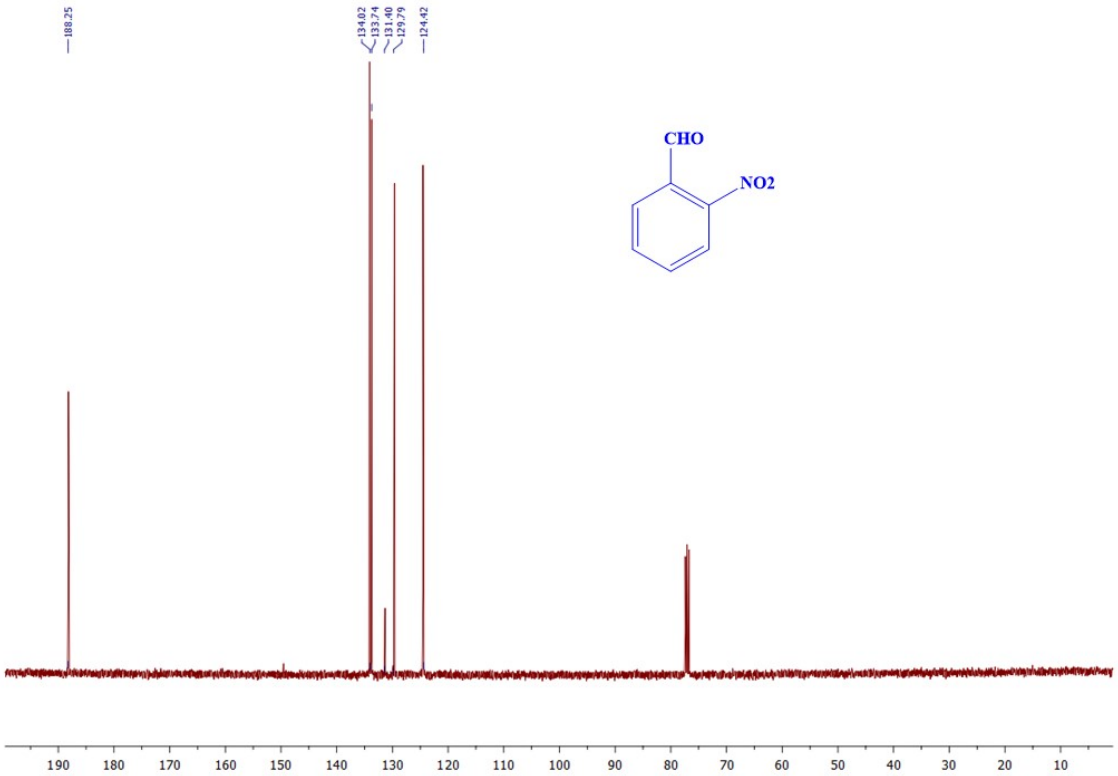

Figure S9.[13]C NMR spectra of **2-nitrobenzaldehyde** in $CDCl_3$.

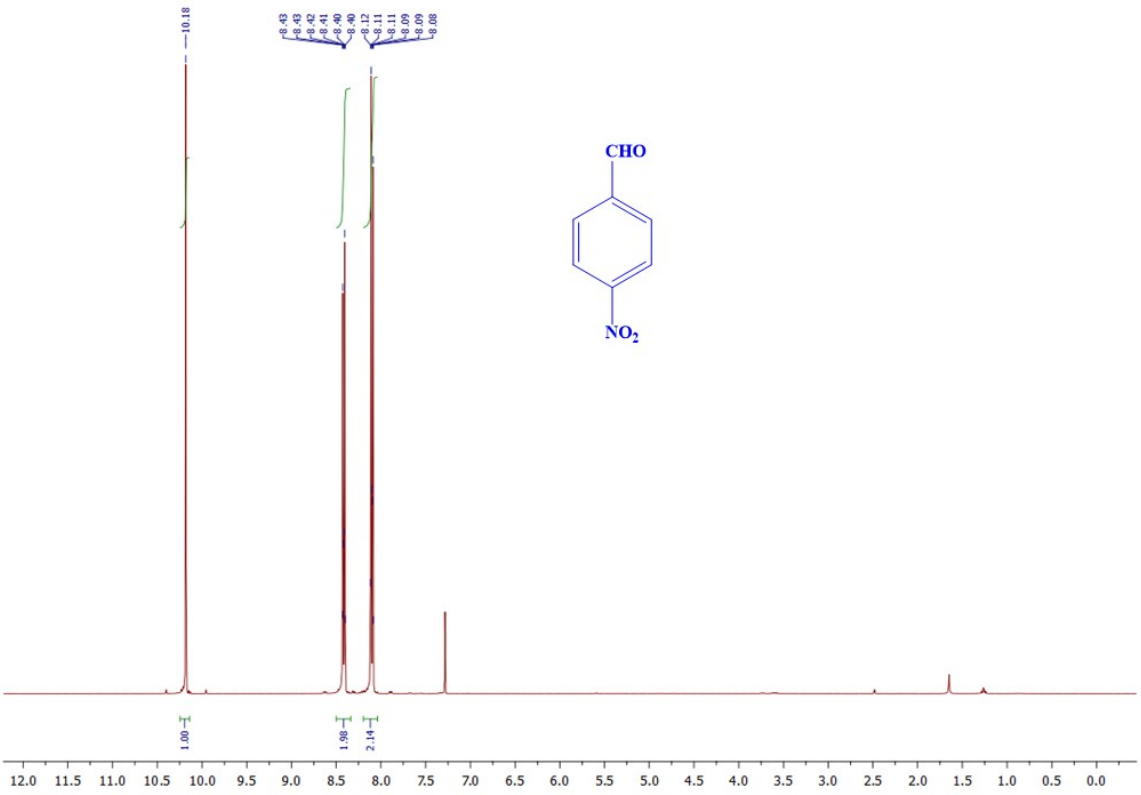

Figure S10.[1]H NMR spectra of **4-nitrobenzaldehyde** in $CDCl_3$.

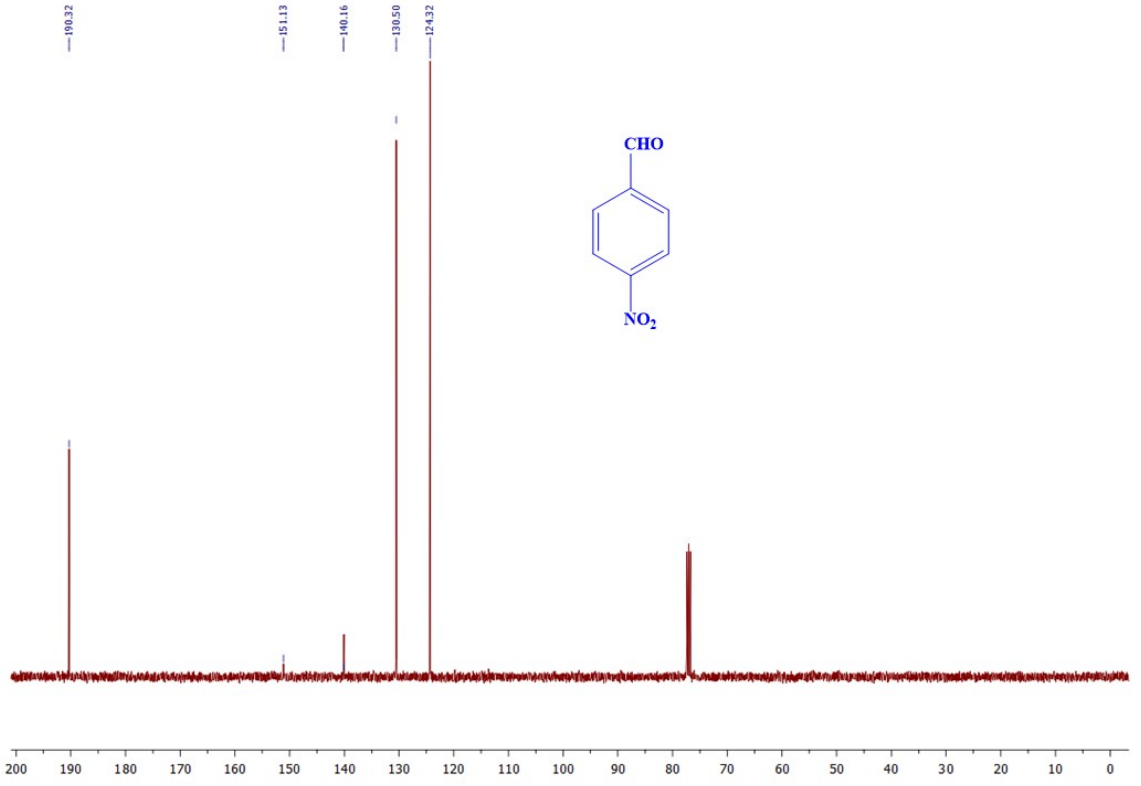

Figure S11.[13]C NMR spectra of **4-nitrobenzaldehyde** in $CDCl_3$.

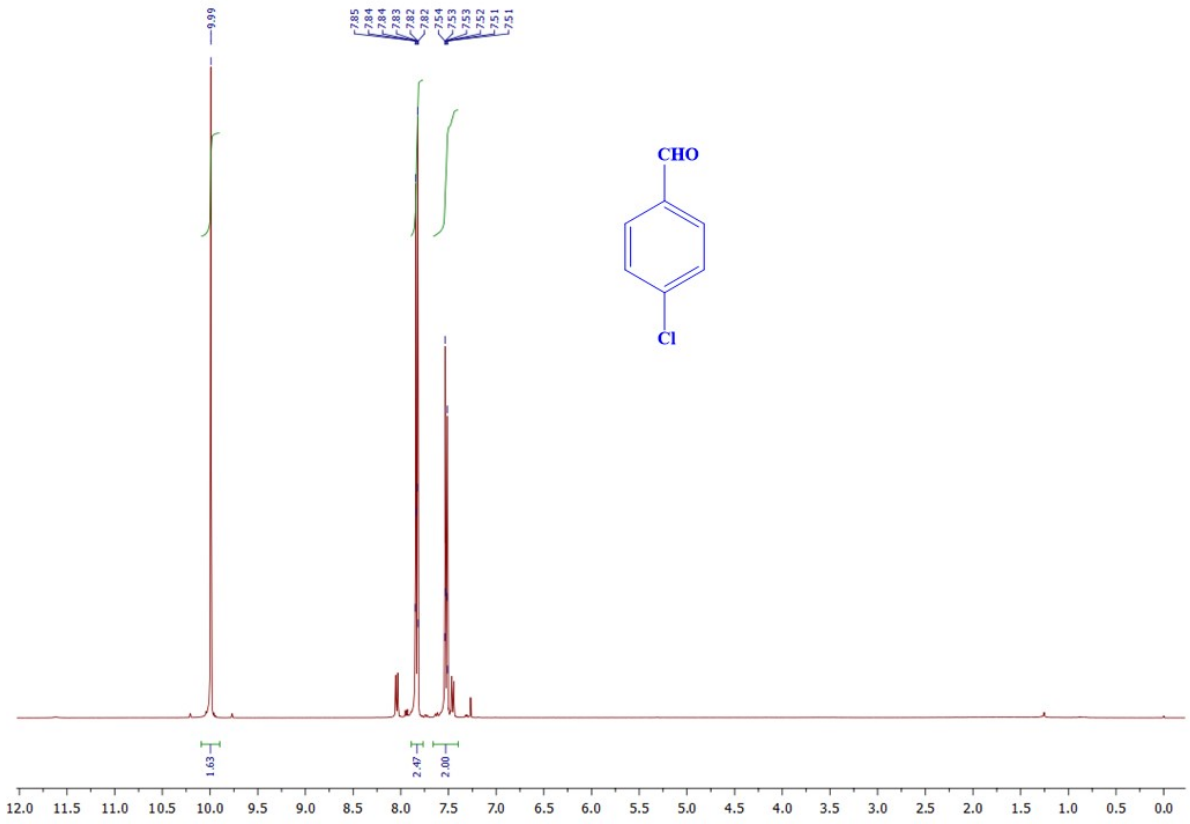

Figure S12. ^{1}H NMR spectra of **4-Chlorobenzaldehyde** in $CDCl_3$.

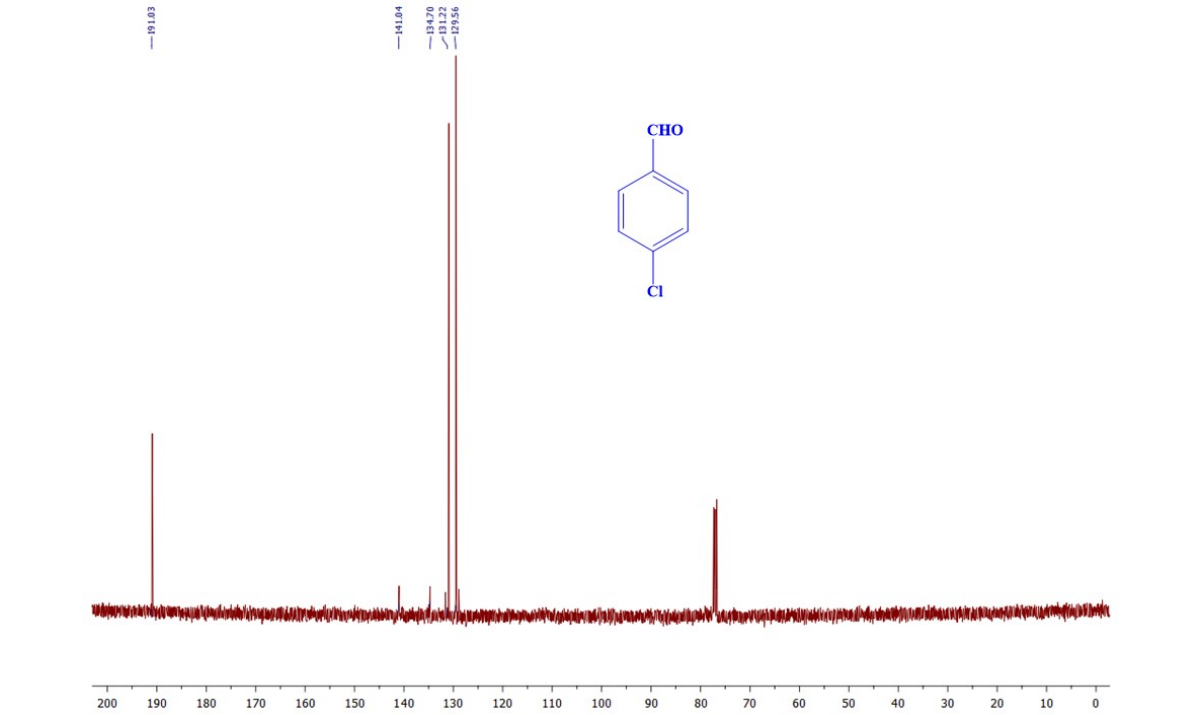

Figure S13. ^{13}C NMR spectra of **4-Chlorobenzaldehyde** in $CDCl_3$.

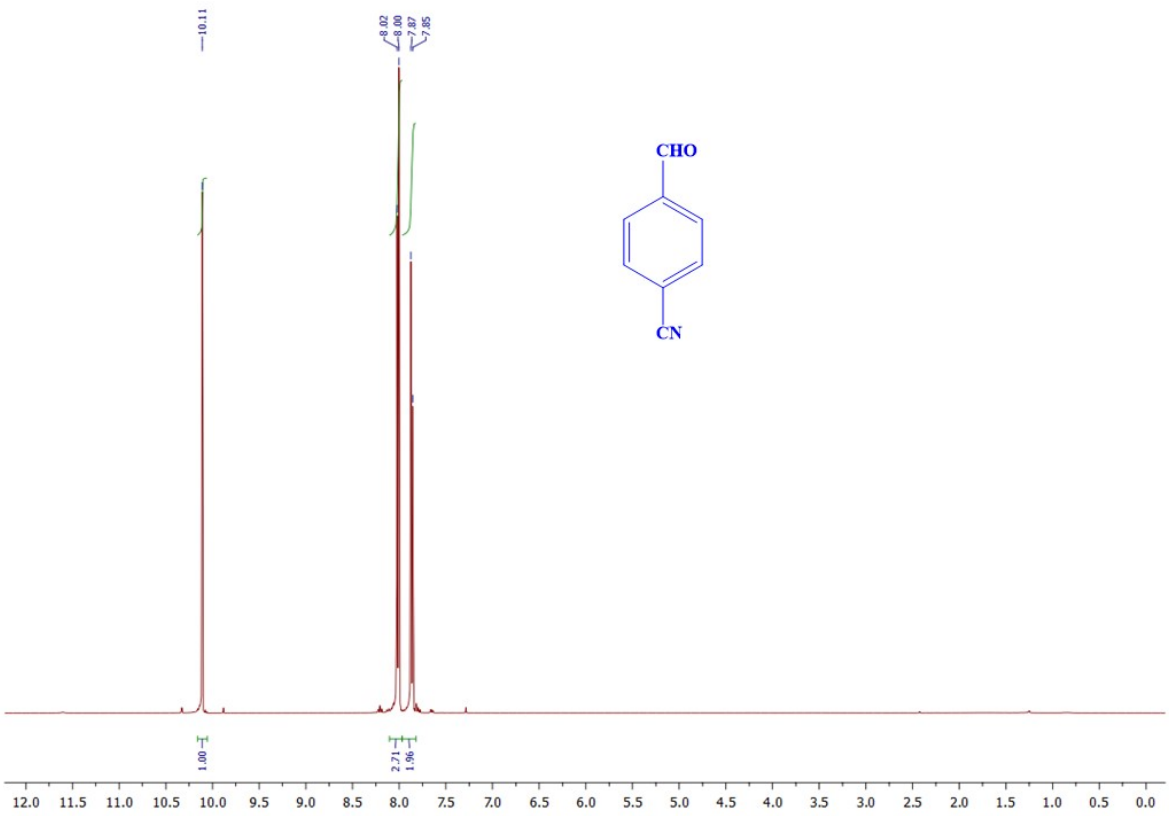

Figure S14.[1]H NMR spectra of **4-formylbenzonitrile** in $CDCl_3$.

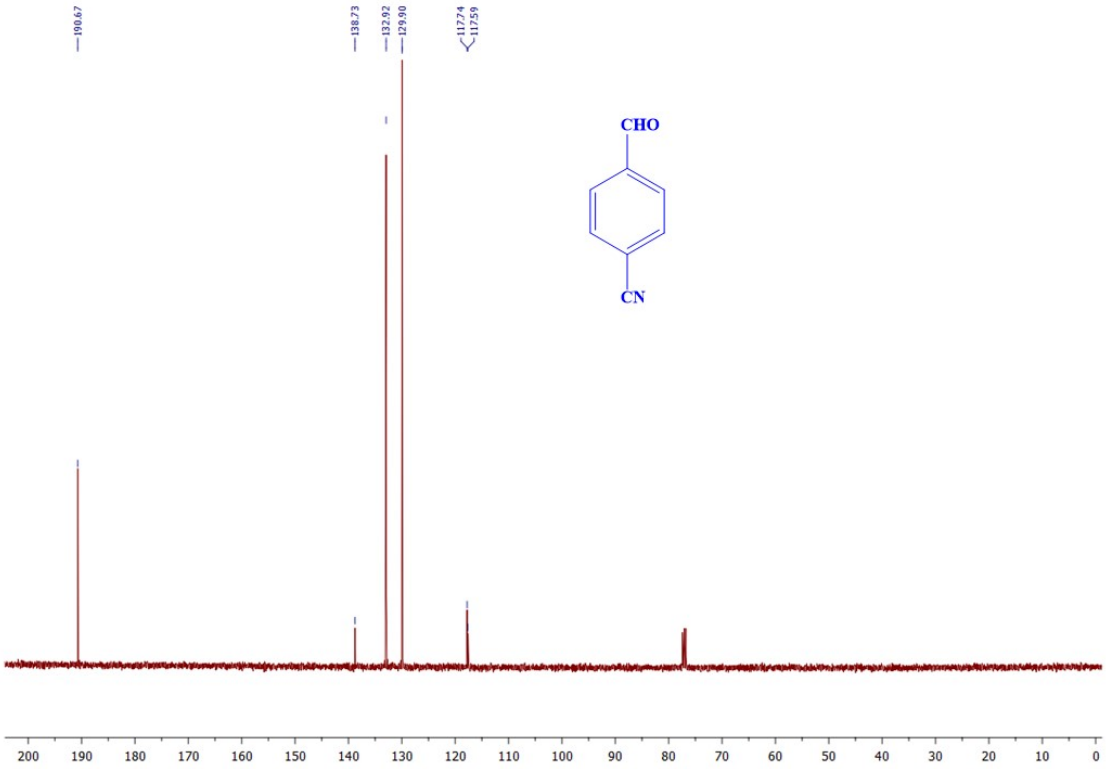

Figure S15.[13]C NMR spectra of **4-formylbenzonitrile** in $CDCl_3$.

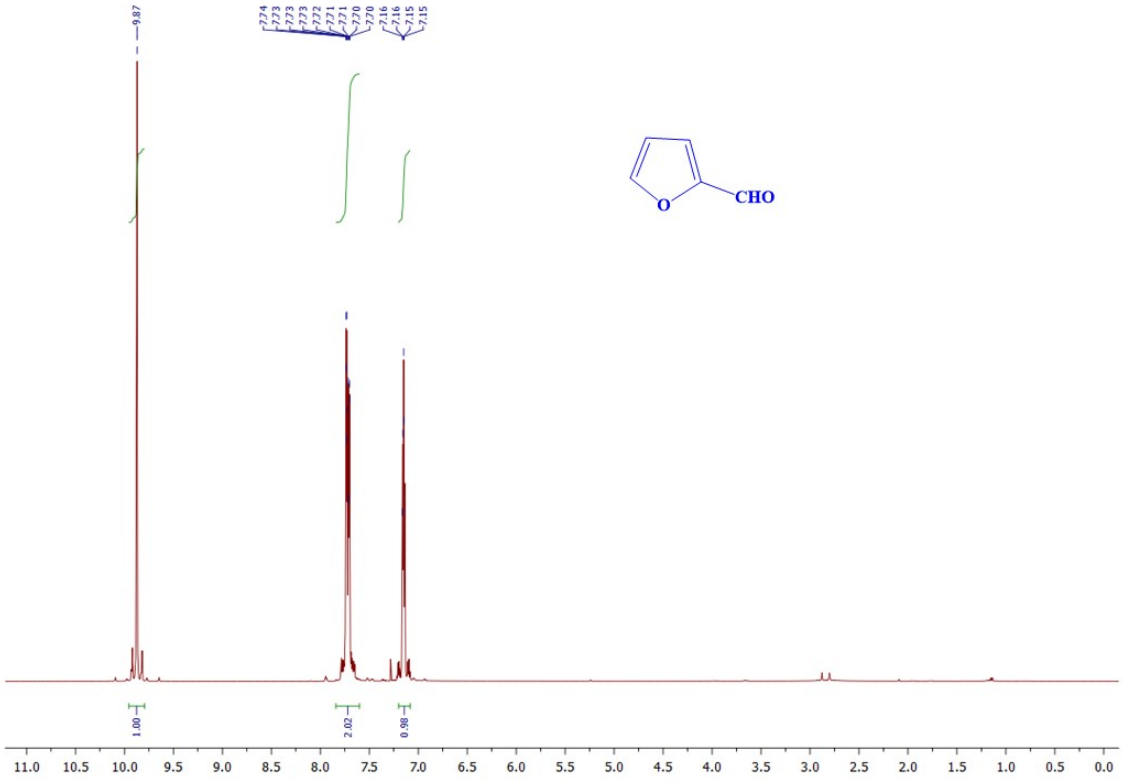

Figure S16. ^{1}H NMR spectra of **furan-2-carbaldehyde** in $CDCl_3$.

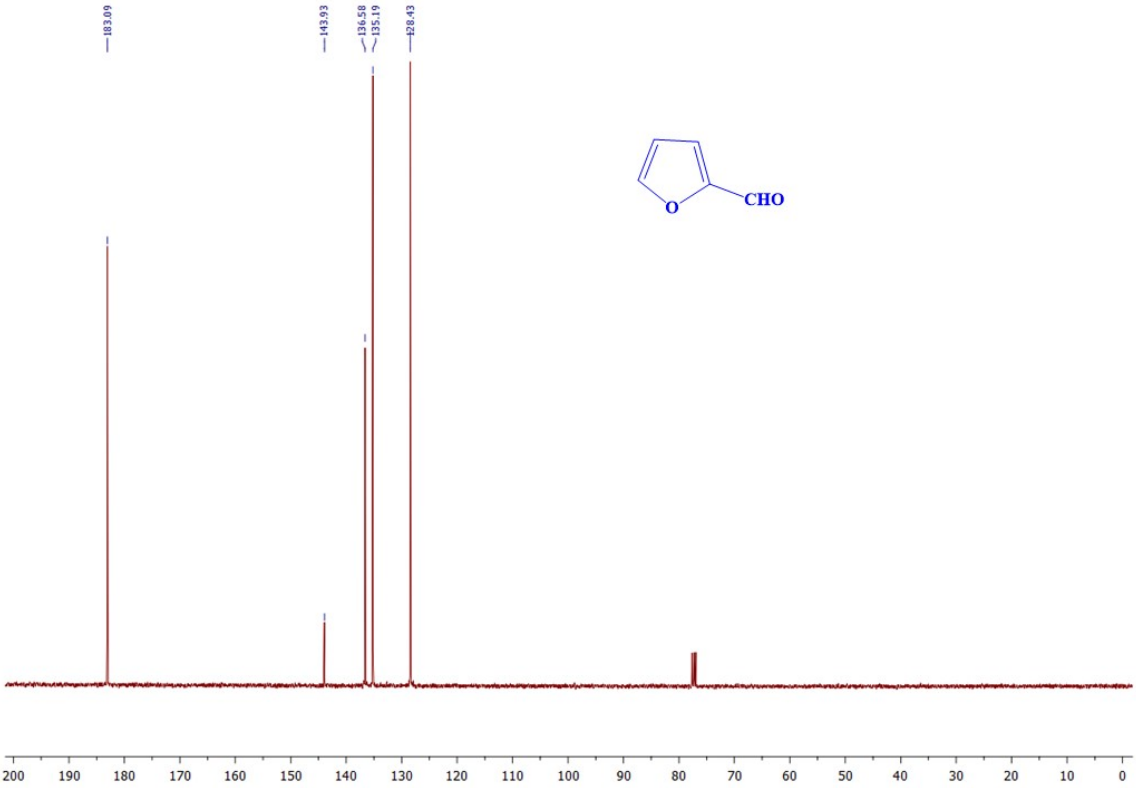

Figure S17. ^{13}C NMR spectra of **furan-2-carbaldehyde** in $CDCl_3$.

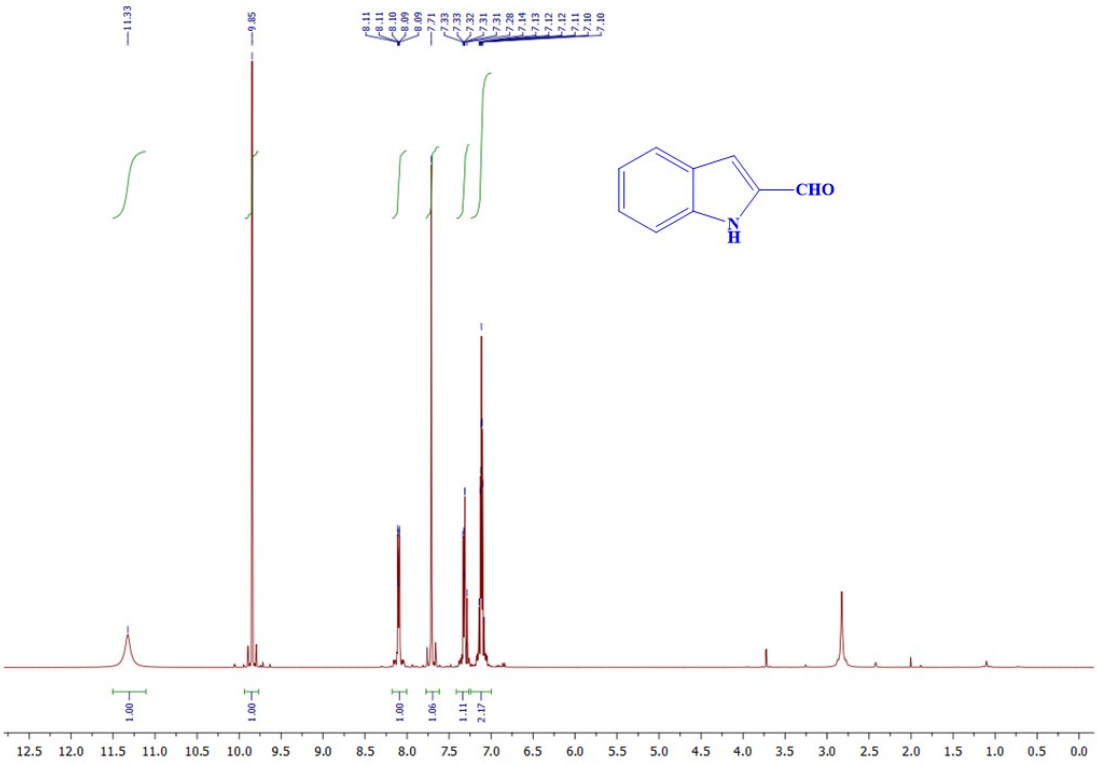

Figure S18.[1]H NMR spectra of **1H-indole-2-carbaldehyde** in DMSO-d_6.

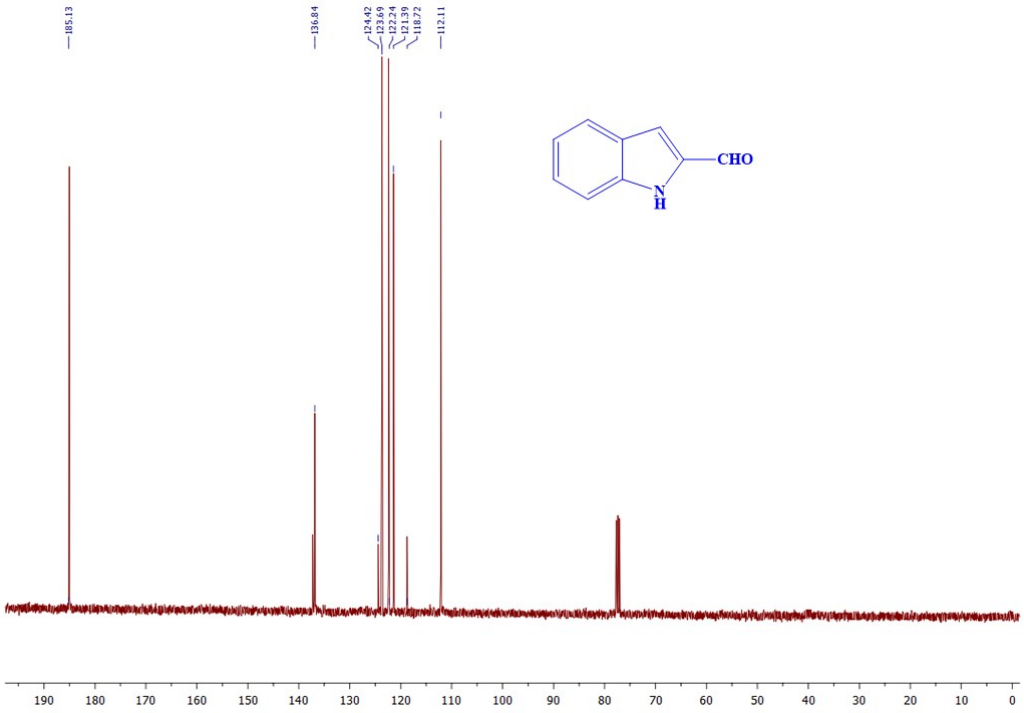

Figure S19.[13]C NMR spectra of **1H-indole-2-carbaldehyde** in $CDCl_3$.

B) FT-IR spectra:

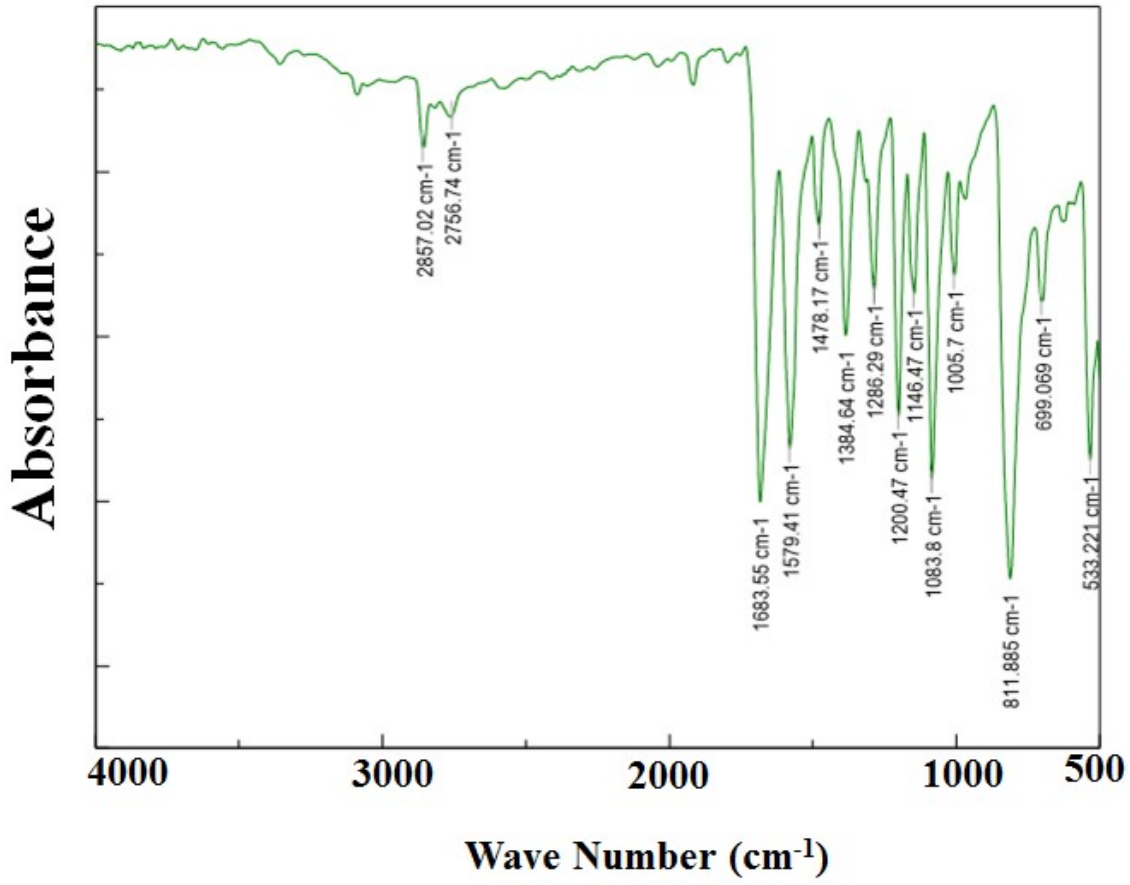

Figure S20. FT-IR spectra of **4-Chlorobenzaldehyde**.

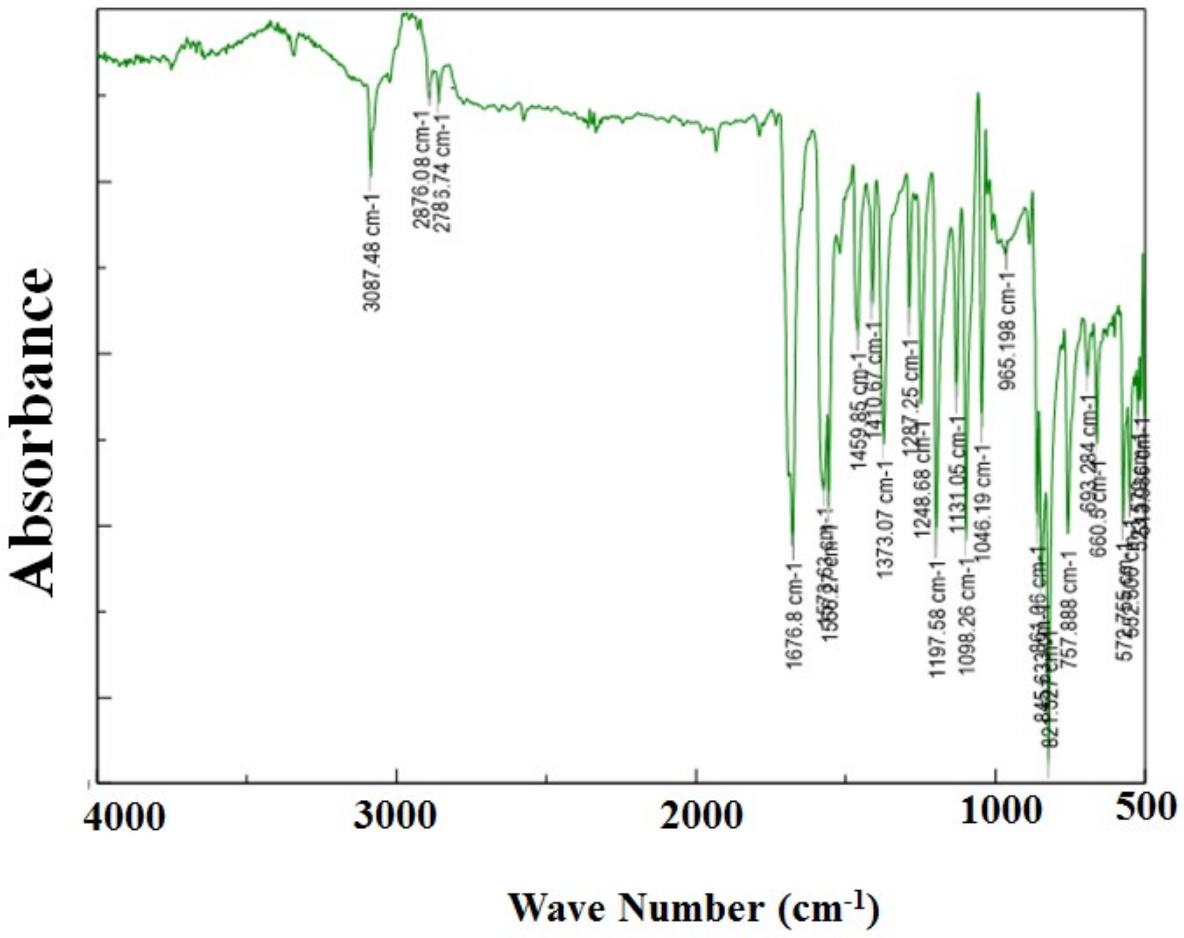

Figure S21. FT-IR spectra of **4-Nitrobenzaldehyde**

References

1. Q. Feng, Q. Song, Aldehydes and Ketones Formation: Copper-Catalyzed Aerobic Oxidative Decarboxylation of Phenylacetic Acids and α-Hydroxyphenylacetic Acids. J. Org. Chem. 79 (2014), 1867-1871.

2. J. H. Kim, K. L. Chan, N. Mahoney, B.C. Campbell, Antifungal Activity of Redox-Active Benzaldehydes that Target Cellular Antioxidation. Ann. Clin. Microbiol. Antimicrob. 10 (2011), 23-37.

3. F. Xi, F. Kamal, M. A. Schenerman, A Novel and Convenient Transformation of Nitriles to Aldehydes. Tetrahedron Lett, 43 (2002), 1395-1396.

4. M. Devi, S. Ganguly, B. Bhuyan, S. Sankar Dhar, S. A. Vadivel, Novel [Fe(acac)$_3$] Interspersed g-C_3N_4 Heterostructure for Environmentally Benign Visible-Light-Driven Oxidation of Alcohols. Eur. J. Inorg. Chem, (2018), 4819-4825.

5. E. E. Stache, A. B. Ertel, T. Rovis, A. G. Doyle, Generation of Phosphoranyl Radicals via Photoredox Catalysis Enables Voltage-Independent Activation of Strong C-O Bonds. ACS. Catal. 8 (2018), 11134-11139.

6. J. L. Liu, Y. C. Chen, Q. W. Li, S. Gomez-Coca, D. Aravena, E. Ruiz, W. Q. Lin, J. D. Leng, M. L. Tong, Two 3d-4f Nanomagnets Formed via a Two-Step insitu Reaction of Picolinaldehyde. *Chem. Commun.* 49 (2013), 6549-6551.

7. N. C. Ganguly, S. K. A. Barik, Facile Mild Deprotection Protocol for 1,3-Dithianes and 1,3-Dithiolanes with 30% Hydrogen Peroxide and Iodine Catalyst in Aqueous Micellar System. Synthesis, (2009), 1393-1399.

8. G. Kumar, F. Hussain, R. Gupta, Copper Based Coordination Polymers based on Metalloligands: Utilization as Heterogeneous Oxidation Catalysts. *Dalton. Trans.* 47 (2018), 16985-16994.